

# Combined Analysis of Processes $\pi\pi \rightarrow \pi\pi, K\bar{K}, \eta\eta$ and $J/\psi$ Decays and Parameters of Scalar Mesons

**Yury S. Surovtsev\***

*Bogoliubov Laboratory of Theoretical Physics, Joint Institute for Nuclear Research, 141 980  
Dubna, Russia*

*E-mail: surovcev@theor.jinr.ru*

**Petr Bydžovský**

*Nuclear Physics Institute, Czech Academy of Sciences, Řež near Prague 25068, Czech Republic*

*E-mail: bydz@ujf.cas.cz*

**Robert Kamiński**

*Institute of Nuclear Physics, Polish Academy of Sciences, Cracow 31342, Poland*

*E-mail: robert.kaminski@ifj.edu.pl*

**Valery E. Lyubovitskij†**

*Institut für Theoretische Physik, Universität Tübingen, Kepler Center for Astro and Particle  
Physics, Auf der Morgenstelle 14, D-72076 Tübingen, Germany*

*E-mail: lubovit@tphys.physik.uni-tuebingen.de*

**Miroslav Nagy**

*Institute of Physics, Slovak Academy of Sciences, Bratislava 84511, Slovak Republic*

*E-mail: miroslav.nagy@savba.sk*

The coupled processes – the  $\pi\pi$  scattering,  $\pi\pi \rightarrow K\bar{K}$ ,  $\pi\pi \rightarrow \eta\eta$  and  $J/\psi \rightarrow \phi\pi\pi, \phi K\bar{K}$  – are considered in the 2- and 3-channel approaches for studying  $f_0$ -mesons. An applied model-independent method of analysis is based on analyticity and unitarity and uses an uniformization procedure. It is shown that for obtaining correct values of the  $f_0$ -meson parameters a one-channel dispersive equation (Roy's equations) analysis of the  $\pi\pi$  scattering is not enough, even for the  $f_0(600)$  which is in the elastic region of the  $\pi\pi$  scattering below the thresholds of coupled channels. At least, the combined 3-channel analysis of data on coupled processes  $\pi\pi \rightarrow \pi\pi, K\bar{K}, \eta\eta$  is needed, which is carried out adding the data on decays  $J/\psi \rightarrow \phi\pi\pi, \phi K\bar{K}$  from Mark III, DM2 and BES Collaborations. The latter allows us considerably to diminish possible scenarios of the resonance representations on the Riemann surface of the  $S$ -matrix, which give the similar description of the multi-channel  $\pi\pi$  scattering and, however, the quite different parameters of some resonances. There are changed most considerably parameters of the  $f_0(600)$  – now the obtained mass is in some accordance with prediction by S. Weinberg on the basis of mended symmetry. Some spectroscopic implications from results of the analysis are discussed.

*XXI International Baldin Seminar on High Energy Physics Problems,*

*September 10-15, 2012*

*JINR, Dubna, Russia*

## 1. Introduction

The problem of interpretation of scalar mesons is tightly related to the most profound topics in particle physics which concern the QCD vacuum. However, parameters of the scalar mesons, their nature and status of some of them are still not well settled [1, 2]. Despite the big effort devoted to studying various aspects of the problem (for recent reviews see, e.g., Refs. [3, 4, 5, 6]) a description of this mesonic sector is far from being complete. For example, applying our model-independent method in the 3-channel analyses of multi-channel  $\pi\pi$  scattering [7, 8], we have obtained parameters of the  $f_0(600)$  and  $f_0(1500)$  which differ considerably from results of analyses utilizing other methods (mainly those based on dispersion relations and Breit-Wigner approaches). Reasons for this difference should be understood because our method of analysis is based only on the demand for analyticity and unitarity of amplitude using a uniformization procedure. The construction of the amplitude is essentially free from any dynamical (model) assumptions utilizing only the *mathematical* fact that a local behaviour of analytic functions determined on the Riemann surface is governed by the nearest singularities on all corresponding sheets, i.e., the obtained parameters of resonances can be considered as free from theoretical prejudice.

In view of indicated circumstances, related to parameters and status of scalar mesons, there are known problems as to determining their QCD nature and assignment to the quark-model configurations. Here we present results of the coupled-channel analysis of data on the isoscalar S-wave processes  $\pi\pi \rightarrow \pi\pi, K\bar{K}, \eta\eta$  and on decays  $J/\psi \rightarrow \pi\pi, K\bar{K}$  for studying  $f_0$ -mesons.

First we explain quite transparently that it is impossible to obtain correct parameters for broad scalar resonances analyzing only the  $\pi\pi$  scattering data as, e.g., in papers [9] – [12]. To this end, we consider the  $\pi\pi$  scattering and the process  $\pi\pi \rightarrow K\bar{K}$  in the 2-channel approach. The point is that in our above-indicated 3-channel analyses, we were enforced to construct the 4-sheeted model of the initial 8-sheeted Riemann surface. This was achieved by neglecting the  $\pi\pi$ -threshold branch-point which means that we have considered the nearest to the physical region semi-sheets of the initial Riemann surface. This is in the line with our approach of a consistent account of the nearest singularities on all relevant sheets. The 2-channel analysis utilizes the full Riemann surface and, therefore, it is free of this approximation and of any suppositions.

Analyzing only the  $\pi\pi$  scattering data when using a 2-channel uniformizing variable, we obtain practically the same values for the resonance parameters as in the above-indicated dispersion relation analyses [9] – [12]. However our approach reveals serious flaws in this case that are successfully cured in the combined 2-channel analysis of the  $\pi\pi \rightarrow \pi\pi, K\bar{K}$  data. In this combined analysis the resonance parameters are inevitably changed and the new values are closer to those in our previous 3-channel analysis, confirming the plausibility of our assumptions in the 3-channel calculations.

Moreover, the remaining pseudo-background in the combined 2-channel analysis of the  $\pi\pi \rightarrow \pi\pi, K\bar{K}$  indicates apparently that it is necessary to allow for at least the  $\eta\eta$  threshold. Therefore we have performed also the combined analysis of the  $\pi\pi \rightarrow \pi\pi, K\bar{K}, \eta\eta$  data using the 3-channel uniformizing variable and adding data on the decays  $J/\psi \rightarrow \pi\pi, K\bar{K}$  from Mark III, DM2 and BES Collaborations [13]. The latter reduces considerably the number of scenarios which are possible

---

\*Speaker.

†On leave of absence from the Department of Physics, Tomsk State University, 634050 Tomsk, Russia

in description of the multi-channel  $\pi\pi$  scattering where some spread in the resonance parameters was obtained. In Conclusions some spectroscopic implications from results of the analysis are discussed.

## 2. Model-independent approach to the 2- and 3-channel $\pi\pi$ scattering

Our model-independent method which essentially utilizes a uniformizing variable can be used only for the 2-channel case and under some conditions for the 3-channel one. Only in these cases we obtain a simple symmetric (easily interpreted) picture of the resonance poles and zeros of the  $S$ -matrix on the uniformization plane. The 2- or 3-channel  $S$ -matrix is determined on the 4- or 8-sheeted Riemann surface, respectively. The matrix elements  $S_{ij}$ , where  $i, j = 1, 2, 3$  denote channels, have the right-hand cuts along the real axis of the  $s$  complex plane ( $s$  is the invariant total energy squared), starting with the channel thresholds  $s_i$  ( $i = 1, 2, 3$ ), and the left-hand cuts. The Riemann-surface sheets are numbered according to the signs of analytic continuations of the square roots  $\sqrt{s - s_i}$  ( $i = 1, 2, 3$ ) as follows:

	I	II	III	IV	V	VI	VII	VIII
$\text{Im}\sqrt{s - s_1}$	+	-	-	+	+	-	-	+
$\text{Im}\sqrt{s - s_2}$	+	+	-	-	-	-	+	+
$\text{Im}\sqrt{s - s_3}$	+	+	+	+	-	-	-	-

Resonance representations on the Riemann surface are obtained using formulas (Table 1) [7, 14] expressing analytic continuations of the  $S$ -matrix elements of the coupled processes to all sheets in terms of those on the physical (I) sheet that have only the resonance zeros (beyond the real axis), at least, around the physical region. Then, starting from the resonance zeros on sheet I, one can obtain an arrangement of poles and zeros of resonance on the whole Riemann surface. In Table 1,

**Table 1:** Analytic continuations of the 3-channel  $S$ -matrix elements to unphysical sheets

Process	I	II	III	IV	V	VI	VII	VIII
$1 \rightarrow 1$	$S_{11}$	$1/S_{11}$	$S_{22}/D_{33}$	$D_{33}/S_{22}$	$\det S/D_{11}$	$D_{11}/\det S$	$S_{33}/D_{22}$	$D_{22}/S_{33}$
$1 \rightarrow 2$	$S_{12}$	$iS_{12}/S_{11}$	$-S_{12}/D_{33}$	$iS_{12}/S_{22}$	$iD_{12}/D_{11}$	$-D_{12}/\det S$	$iD_{12}/D_{22}$	$D_{12}/S_{33}$
$2 \rightarrow 2$	$S_{22}$	$D_{33}/S_{11}$	$S_{11}/D_{33}$	$1/S_{22}$	$S_{33}/D_{11}$	$D_{22}/\det S$	$\det S/D_{22}$	$D_{11}/S_{33}$
$1 \rightarrow 3$	$S_{13}$	$iS_{13}/S_{11}$	$-iD_{13}/D_{33}$	$-D_{13}/S_{22}$	$-iD_{13}/D_{11}$	$D_{13}/\det S$	$-S_{13}/D_{22}$	$iS_{13}/S_{33}$
$2 \rightarrow 3$	$S_{23}$	$D_{23}/S_{11}$	$iD_{23}/D_{33}$	$iS_{23}/S_{22}$	$-S_{23}/D_{11}$	$-D_{23}/\det S$	$iD_{23}/D_{22}$	$iS_{23}/S_{33}$
$3 \rightarrow 3$	$S_{33}$	$D_{22}/S_{11}$	$\det S/D_{33}$	$D_{11}/S_{22}$	$S_{22}/D_{11}$	$D_{33}/\det S$	$S_{11}/D_{22}$	$1/S_{33}$

the superscript  $I$  is omitted to simplify the notation,  $\det S$  is the determinant of the  $3 \times 3$   $S$ -matrix on sheet I,  $D_{\alpha\beta}$  is the minor of the element  $S_{\alpha\beta}$ , that is,  $D_{11} = S_{22}S_{33} - S_{23}^2$ ,  $D_{22} = S_{11}S_{33} - S_{13}^2$ ,  $D_{33} = S_{11}S_{22} - S_{12}^2$ ,  $D_{12} = S_{12}S_{33} - S_{13}S_{23}$ ,  $D_{23} = S_{11}S_{23} - S_{12}S_{13}$ , etc.

In the 2-channel case, three types of resonances are obtained corresponding to a pair of conjugate zeros on sheet I only in  $S_{11}$  – the type (a), only in  $S_{22}$  – (b), and simultaneously in  $S_{11}$  and  $S_{22}$  – (c).

In the 3-channel case, we obtain seven types of resonances corresponding to seven possible situations when there are resonance zeros on sheet I only in  $S_{11}$  – (a);  $S_{22}$  – (b);  $S_{33}$  – (c);  $S_{11}$  and  $S_{22}$  – (d);  $S_{22}$  and  $S_{33}$  – (e);  $S_{11}$  and  $S_{33}$  – (f);  $S_{11}$ ,  $S_{22}$  and  $S_{33}$  – (g). The resonance of every type is represented by the pair of complex-conjugate clusters (of poles and zeros on the Riemann surface).

A necessary and sufficient condition for existence of the multi-channel resonance is its representation by one of the types of pole clusters. A main model-independent contribution of resonances is given by the pole clusters and possible remaining small (model-dependent) contributions of resonances can be included in the background. This is confirmed further by the obtained simple description of the background.

The cluster type is related to the nature of state. E.g., if we consider the  $\pi\pi$ ,  $K\bar{K}$  and  $\eta\eta$  channels, then a resonance, coupled relatively more strongly to the  $\pi\pi$  channel than to the  $K\bar{K}$  and  $\eta\eta$  ones is described by the cluster of type (a). In the opposite case, it is represented by the cluster of type (e) (say, the state with the dominant  $s\bar{s}$  component). The glueball must be represented by the cluster of type (g) (of type (c) in the 2-channel consideration) as a necessary condition for the ideal case.

Whereas cases (a), (b) and (c) can be related to the resonance representation by Breit-Wigner forms, cases (d), (e), (f) and (g) practically are lost at the Breit-Wigner description.

One can formulate a model-independent test as a necessary condition to distinguish a bound state of colorless particles (e.g., a  $K\bar{K}$  molecule) and a  $q\bar{q}$  bound state [14, 15]. In the 1-channel case, the existence of the particle bound-state means the presence of a pole on the real axis under the threshold on the physical sheet. In the 2-channel case, existence of the bound-state in channel 2 ( $K\bar{K}$  molecule) that, however, can decay into channel 1 ( $\pi\pi$  decay), would imply the presence of the pair of complex conjugate poles on sheet II under the second-channel threshold without the corresponding shifted pair of poles on sheet III. In the 3-channel case, the bound state in channel 3 ( $\eta\eta$ ) that, however, can decay into channels 1 ( $\pi\pi$  decay) and 2 ( $K\bar{K}$  decay), is represented by the pair of complex conjugate poles on sheet II and by the pair of shifted poles on sheet III under the  $\eta\eta$  threshold without the corresponding poles on sheets VI and VII. According to this test, earlier we rejected interpretation of the  $f_0(980)$  as the  $K\bar{K}$  molecule because this state is represented by the cluster of type (a) in the 2-channel analysis of processes  $\pi\pi \rightarrow \pi\pi, K\bar{K}$  and, therefore, does not satisfy the necessary condition to be the  $K\bar{K}$  molecule [14].

It is convenient to use the Le Couteur-Newton relations [16]. They express the  $S$ -matrix elements of all coupled processes in terms of the Jost matrix determinant  $d(\sqrt{s-s_1}, \dots, \sqrt{s-s_n})$  that is a real analytic function with the only branch-points at  $\sqrt{s-s_i} = 0$ . The important branch points, corresponding to the thresholds of the coupled channels and to the crossing ones, are taken into account in the proper uniformizing variable.

For the data on multi-channel  $\pi\pi$  scattering we used the results of phase analyses which are given for phase shifts of the amplitudes  $\delta_{\alpha\beta}$  and for the modules of the  $S$ -matrix elements  $\eta_{\alpha\beta} = |S_{\alpha\beta}|$  ( $\alpha, \beta = 1, 2, 3$ ):

$$S_{\alpha\alpha} = \eta_{\alpha\alpha} e^{2i\delta_{\alpha\alpha}}, \quad S_{\alpha\beta} = \eta_{\alpha\beta} e^{i\phi_{\alpha\beta}}. \quad (2.1)$$

If below the third threshold there is the 2-channel unitarity then the relations

$$\eta_{11} = \eta_{22}, \quad \eta_{12} = (1 - \eta_{11}^2)^{1/2}, \quad \phi_{12} = \delta_{11} + \delta_{22} \quad (2.2)$$

are fulfilled in this energy region.

For the  $\pi\pi$  scattering, the data from the threshold to 1.89 GeV are taken from [17]. For the process  $\pi\pi \rightarrow K\bar{K}$ , practically all the accessible data are used [18]. For  $\pi\pi \rightarrow \eta\eta$ , we used data for  $|S_{13}|^2$  from the threshold to 1.72 GeV [19].

Here the combined 2- and 3-channel analyses of the coupled processes are carried out assuming that in the 1500-MeV region two states – wide and narrow – exist.

### 3. The 2-channel analysis of data on isoscalar S-wave processes $\pi\pi \rightarrow \pi\pi, K\bar{K}$

#### 3.1 The 2-channel analysis only of the $\pi\pi$ -scattering data

In the 2-channel analysis of processes  $\pi\pi \rightarrow \pi\pi, K\bar{K}$  we applied the uniformizing variable which takes into account, in addition to the  $\pi\pi$ - and  $K\bar{K}$ -threshold branch-points, the left-hand branch-point at  $s = 0$ , related to the  $\pi\pi$  crossed channels:

$$v = \frac{\sqrt{(s-s_1)s_2} + \sqrt{(s-s_2)s_1}}{\sqrt{s(s_2-s_1)}} \quad (s_1 = 4m_\pi^2 \text{ and } s_2 = 4m_K^2). \quad (3.1)$$

It maps the 4-sheeted Riemann surface with two unitary cuts and the left-hand cut onto the  $v$ -plane. In Figure 1, there are shown an uniformization  $v$ -plane for the 2-channel- $\pi\pi$ -scattering amplitude and the representation of resonances of types **(a)**, **(b)** and **(c)**: the Roman numerals (I, ..., IV) denote the images of the corresponding sheets; the thick line represents the physical region; the points  $i$ , 1 and  $b = \sqrt{(m_K + m_\pi)/(m_K - m_\pi)}$  correspond to the  $\pi\pi, K\bar{K}$  thresholds and  $s = \infty$ , respectively; the shaded intervals  $(-\infty, -b]$ ,  $[-b^{-1}, b^{-1}]$ ,  $[b, \infty)$  are the images of the corresponding edges of the left-hand cut. The depicted positions of poles (+) and of zeros (o) give the resonance representations of the type **(a)**, **(b)** and **(c)** in  $S_{11}$ .

On the  $v$ -plane,  $S_{11}(v)$  has no cuts;  $S_{12}^2(v)$  and  $S_{22}(v)$  do have the cuts which arise from the left-hand cut on the  $s$ -plane, starting at  $s = 4(m_K^2 - m_\pi^2)$ . Further the contribution of the left-hand cut is approximated by a pole

$$d_L = v^{-4}(1 - (p - i\sqrt{1-p^2})v)^4(1 + (p + i\sqrt{1-p^2})v)^4, \quad (3.2)$$

where  $p = 0.903 \pm 0.0004$  from the analysis. The 4th power is stipulated by the following model-independent arguments. First, a pole on the real  $s$ -axis on the physical sheet in  $S_{22}$  is accompanied by a pole on sheet II at the same  $s$ -value. On the  $v$ -plane this implies the pole of 2nd order (and also zero of the same order, symmetric to the pole with respect to the real axis). Second, for the  $s$ -channel process  $\pi\pi \rightarrow K\bar{K}$ , the crossing  $u$ - and  $t$ -channels are the  $\pi - K$  and  $\bar{\pi} - K$  scattering (exchanges in these channels give contributions on the left-hand cut). This results in the additional doubling of the multiplicity of the indicated pole on the  $v$ -plane. Therefore, the contribution of the left-hand cut is approximated as the fourth-power pole on the real  $s$ -axis on sheet I in the sub- $K\bar{K}$ -threshold region. On the  $v$ -plane, the Le Couteur-Newton relations are

$$S_{11} = \frac{d(-v^{-1})}{d(v)}, \quad S_{22} = \frac{d(v^{-1})}{d(v)}, \quad S_{11}S_{22} - S_{12}^2 = \frac{d(-v)}{d(v)}. \quad (3.3)$$

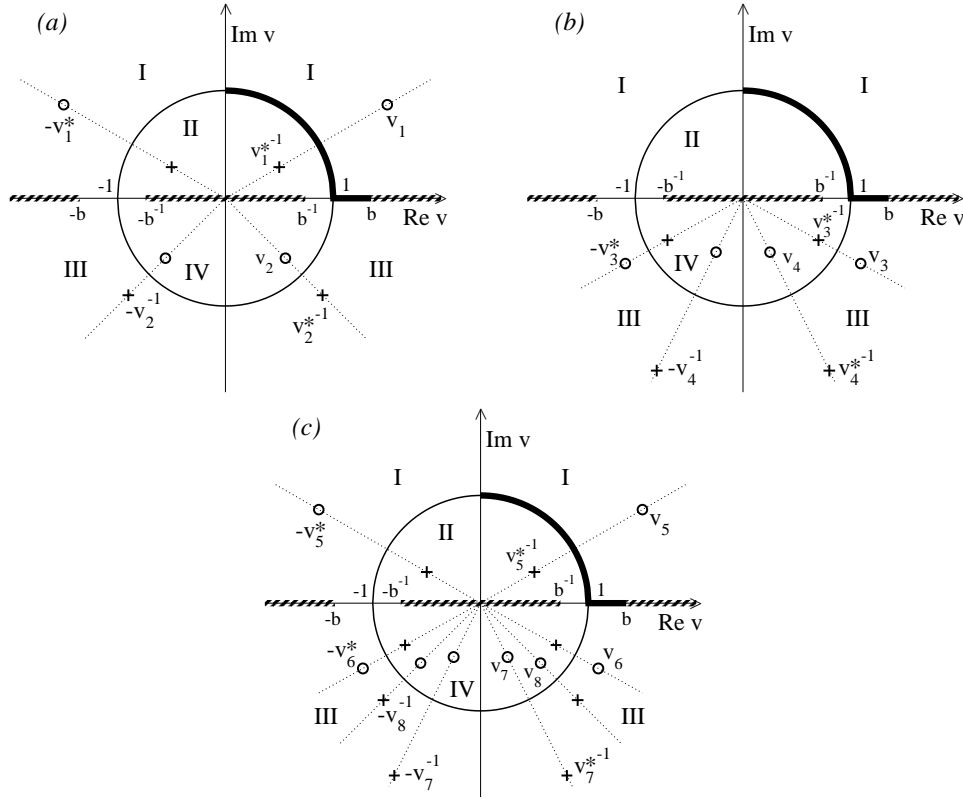


**Figure 1:** Representation of resonances of type (a), (b) and (c) on the uniformization  $v$ -plane in  $S_{11}$  in the 2-channel approach are shown in panels (a), (b) and (c), respectively.

Now  $d(v) = d_{res}d_Ld_{bg}$  does not possess already branch points. The  $d_{res}(v)$  represents the contribution of resonances:

$$d_{res} = v^{-M} \prod_{n=1}^M (1 - v_n^* v)(1 + v_n v), \quad (3.4)$$

where  $M$  is the number of pairs of the conjugate zeros. The background part is

$$d_{bg} = \exp\left[-i \sum_{n=1}^3 \frac{\sqrt{s-s_n}}{2m_n} (\alpha_n + i\beta_n)\right] \quad (3.5)$$

with

$$\alpha_n = a_{n1} + a_{n\eta} \frac{s-s_\eta}{s_\eta} \theta(s-s_\eta) + a_{n\sigma} \frac{s-s_\sigma}{s_\sigma} \theta(s-s_\sigma) + a_{nv} \frac{s-s_v}{s_v} \theta(s-s_v) \quad (3.6)$$

$$\beta_n = b_{n1} + b_{n\eta} \frac{s-s_\eta}{s_\eta} \theta(s-s_\eta) + b_{n\sigma} \frac{s-s_\sigma}{s_\sigma} \theta(s-s_\sigma) + b_{nv} \frac{s-s_v}{s_v} \theta(s-s_v) \quad (3.7)$$

where  $s_\eta$  and  $s_\sigma$  are the  $\eta\eta$  and  $\sigma\sigma$  thresholds, respectively;  $s_v$  is a combined threshold of  $\eta\eta'$ ,  $\rho\rho$  and  $\omega\omega$  channels in the vicinity of 1.5 GeV. From the analysis:  $s_\sigma = 1.6558 \text{ GeV}^2$ ,  $s_v = 2.1293 \text{ GeV}^2$ .

Initially analyzing only the  $\pi\pi$  scattering, we achieved an excellent description of the data for  $\delta_{11}$  and modulus of the  $S$ -matrix element (the total  $\chi^2/\text{NDF} = 171.715/(189 - 29) \approx 1.07$ ).

Obtained parameters of resonances (Table 2) largely coincide with the values cited as estimations of the PDG [1, 2], though a negative phase-shift in the background at the  $\pi\pi$  threshold arises.

**Table 2:** Pole clusters for resonances on the complex  $\sqrt{s}$ -plane in the analysis of only  $\pi\pi$ -scattering. Pole positions  $\sqrt{s_r} = E_r - i\Gamma_r/2$  in MeV are shown.

Sheet		II	III	IV
$f_0(600)$	$E_r$	$447.5 \pm 5.9$	$492.7 \pm 36.0$	
	$\Gamma_r/2$	$267.0 \pm 6.5$	$307.8 \pm 16.5$	
$f_0(980)$	$E_r$	$1001.1 \pm 3.7$	$979.1 \pm 12.0$	
	$\Gamma_r/2$	$20.3 \pm 2.6$	$38.5 \pm 7.1$	
$f_0(1370)$	$E_r$		$1375.8 \pm 51.5$	$1301.1 \pm 47.9$
	$\Gamma_r/2$		$179.5 \pm 36.5$	$224.0 \pm 49.3$
$f_0(1500)$	$E_r$		$1498.8 \pm 39.3$	$1503.7 \pm 45.1$
	$\Gamma_r/2$		$51.8 \pm 43.3$	$56.5 \pm 39.4$
$f'_0(1500)$	$E_r$	$1511.4 \pm 11.2$	$1499.8 \pm 104.3$ $1509.1 \pm 119.4$	$1505.9 \pm 38.5$
	$\Gamma_r/2$	$200.5 \pm 11.0$	$310.5 \pm 58.8$ $241.0 \pm 63.8$	$168.1 \pm 40.6$
$f_0(1710)$	$E_r$		$1700.3 \pm 31.2$	$1720.1 \pm 32.2$
	$\Gamma_r/2$		$58.6 \pm 26.4$	$64.9 \pm 30.1$

In the analysis, the  $f_0(600)$  and  $f_0(980)$  are described by the pole clusters of type (a);  $f_0(1370)$ ,  $f_0(1500)$  and  $f_0(1710)$ , type (b);  $f'_0(1500)$ , type (c).

The received background parameters are:  $a_{11} = -0.0895 \pm 0.0030$ ,  $a_{1\eta} = 0.04 \pm 0.03$ ,  $a_{1\sigma} = 0.0 \pm 0.8$ ,  $a_{1\nu} = 0.0 \pm 0.7$ ,  $b_{11} = 0.0 \pm 0.007$ ,  $b_{1\eta} = 0.0 \pm 0.01$ ,  $b_{1\sigma} = 0.0 \pm 0.02$ ,  $b_{1\nu} = 0.054 \pm 0.036$ .

For the  $f_0(600)$  the found pole on sheet II coincides practically with the value  $450 - i275$  MeV which was found in the dispersive  $\pi\pi$ -scattering data analyses which considered the region from the threshold to  $1400 \div 1500$  MeV [9, 10]. The parameters of the  $f_0(1370)$ , narrow  $f_0(1500)$  and  $f_0(1710)$  are very near to the estimations of the PDG [1, 2]. More remarkable differences were only for the mass of  $f_0(980)$  (1001 MeV against  $980 \pm 10$  MeV of the PDG tables of 2010) and the existence the wide  $f'_0(1500)$ . However, the mass of  $f_0(980)$  slightly above 1 GeV was also obtained in other works which analyzed the  $\pi\pi$  scattering (e.g. [12]). In the quite recent PDG tables of 2012, for the mass of  $f_0(980)$  there is indicated already the estimation  $990 \pm 20$  MeV [2].

The obtained  $\pi\pi$  scattering length  $a_0^0 = 0.222 \pm 0.008 m_{\pi^+}^{-1}$  is also in the very good agreement with the experimental results and with the ChPT calculations.

However, this analysis displays two important flaws:

1. The negative phase-shift in the background beginning from the  $\pi\pi$  threshold ( $a_{11} = -0.0895$ ) is necessary for a successful description of the data. This should not be the case because, in the uniformizing variable, we have taken into account the left-hand branch-point at  $s = 0$

which gives a main contribution to the  $\pi\pi$  background below the  $K\bar{K}$  threshold. Other possible contributions of the left-hand cut related with exchanges by the nearest mesons – the  $\rho$ -meson and the  $f_0(600)$  – practically obliterate each other [20] because vector and scalar particles contribute with the opposite signs due to the gauge invariance.

2. The description of the data on reaction  $\pi\pi \rightarrow K\bar{K}$ , using the same parameters of resonances as in the  $\pi\pi$  channel, is satisfactory only for the phase shift  $\phi_{12}$  which is due to the approximation of the left-hand cut in  $S_{12}$  and  $S_{22}$ , beginning at  $s = 4(m_K^2 - m_\pi^2)$ , by the 4th-power pole on the  $\nu$ -plane. The module of the  $S$ -matrix element  $\eta_{12}$  is described well only from the  $K\bar{K}$  threshold up to about 1.15 GeV as it should be due to the “elastic” two-channel unitarity. Above this energy the description fails even qualitatively.

We conclude: If the data are consistent, for obtaining more correct parameters of wide resonances the combined analysis of data on coupled processes  $\pi\pi \rightarrow \pi\pi, K\bar{K}$  is needed. Further that analysis is performed.

### 3.2 The combined 2-channel analysis of the $\pi\pi \rightarrow \pi\pi, K\bar{K}$ data

The resonances in this analysis are described by pole clusters of the same types as in the analysis only of the  $\pi\pi$  scattering: the  $f_0(600)$  and  $f_0(980)$  are represented by the clusters of type (a);  $f_0(1370)$ ,  $f_0(1500)$  and  $f_0(1710)$ , type (b);  $f'_0(1500)$ , type (c).

The data for the  $\pi\pi$  scattering below 1 GeV admit two satisfactory solutions for the phase shift – A and B – which mutually differ mainly in the pole position on sheet II for the  $f_0(600)$ . The total  $\chi^2/\text{NDF}$  is  $416.887/(312 - 40) \approx 1.53$  for the A-solution and  $\approx 1.44$  for the B-solution.

The obtained background parameters for the A-solution are:

$$\underline{a_{11} = 0.0 \pm 0.003, a_{1\eta} = -0.1004 \pm 0.0301, a_{1\sigma} = 0.2148 \pm 0.0822, a_{1\nu} = 0.0 \pm 0.07, b_{11} = b_{1\eta} = b_{1\sigma} = 0, b_{1\nu} = 0.012 \pm 0.0287, a_{21} = -0.919 \pm 0.107, a_{2\eta} = -1.399 \pm 0.348, a_{2\sigma} = 0.0 \pm 0.7, a_{2\nu} = -11.45 \pm 0.75, b_{21} = 0.0747 \pm 0.0503, b_{2\eta} = b_{2\sigma} = 0, b_{2\nu} = 4.83 \pm 1.94;}$$

for B-solution:

$$\underline{a_{11} = 0.0 \pm 0.003, a_{1\eta} = -0.0913 \pm 0.0327, a_{1\sigma} = 0.1707 \pm 0.0899, a_{1\nu} = 0.0 \pm 0.07, b_{11} = b_{1\eta} = b_{1\sigma} = 0, b_{1\nu} = 0.006 \pm 0.029, a_{21} = -1.338 \pm 0.111, a_{2\eta} = -1.119 \pm 0.376, a_{2\sigma} = 0.0 \pm 0.8, a_{2\nu} = -12.13 \pm 0.77, b_{21} = 0.018 \pm 0.050, b_{2\eta} = b_{2\sigma} = 0, b_{2\nu} = 4.48 \pm 1.98.}$$

Further in Table 3, the obtained pole-clusters for resonances are shown on the  $\sqrt{s}$ -plane for the A- and B-solutions.

In Figures 2, we show energy behaviour of the phase shifts and modules of the  $S$ -matrix elements for the  $\pi\pi$ -scattering and  $\pi\pi \rightarrow K\bar{K}$ , obtained in the analysis only of  $\pi\pi$ -scattering and in the combined analysis of processes  $\pi\pi \rightarrow \pi\pi, K\bar{K}$  and compared with the experimental data.

In Table 4 we compare our results for the  $\pi\pi$  scattering length  $a_0^0$ , obtained in the analyses, with results of some other theoretical and experimental works. We stress that in case when we restrict to the analysis of the  $\pi\pi$  scattering and in case of the A-solution (lower mass and width of  $f_0(600)$  meson) we reproduce with a high accuracy the results of the chiral perturbation theory (ChPT) [9, 21] including constraints imposed by the Roy’s equations. On the other side, the B-solution (with a heavier mass and width of  $f_0(600)$  meson) is similar to the the predictions of the

**Table 3:** Pole clusters for resonances on the complex  $\sqrt{s}$ -plane in the combined analysis of processes  $\pi\pi \rightarrow \pi\pi, K\bar{K}$ . Pole positions  $\sqrt{s}_r = E_r - i\Gamma_r/2$  in MeV are shown.

Solution	Sheet		II	III	IV
A	$f_0(600)$	$E_r$	$517.0 \pm 7.8$	$458.5 \pm 14.7$	
		$\Gamma_r/2$	$393.9 \pm 6.0$	$205.9 \pm 4.7$	
	$f_0(980)$	$E_r$	$1004.6 \pm 3.9$	$995.5 \pm 10.1$	
		$\Gamma_r/2$	$25.0 \pm 2.3$	$96.9 \pm 2.7$	
	$f_0(1370)$	$E_r$		$1351.5 \pm 32.5$	$1342.9 \pm 12.2$
		$\Gamma_r/2$		$369.0 \pm 45.7$	$221.6 \pm 30.7$
$f_0(1500)$	$E_r$		$1498.7 \pm 5.8$	$1501.1 \pm 6.4$	
	$\Gamma_r/2$		$56.7 \pm 5.6$	$56.6 \pm 6.0$	
$f'_0(1500)$	$E_r$	$1532.2 \pm 12.4$	$1489.1 \pm 16.2$	$1515.9 \pm 29.2$	$1519.3 \pm 18.7$
	$\Gamma_r/2$	$323.2 \pm 21.0$	$217.9 \pm 10.2$	$388.4 \pm 22.6$	$339.5 \pm 42.2$
$f_0(1710)$	$E_r$		$1701.9 \pm 31.8$		$1717.0 \pm 34.9$
	$\Gamma_r/2$		$77.8 \pm 18.0$		$72.9 \pm 16.2$
B	$f_0(600)$	$E_r$	$550.6 \pm 9.0$	$664.5 \pm 12.1$	
		$\Gamma_r/2$	$502.1 \pm 7.2$	$188.2 \pm 2.6$	
	$f_0(980)$	$E_r$	$1003.2 \pm 3.0$	$995.4 \pm 7.3$	
		$\Gamma_r/2$	$28.9 \pm 2.0$	$96.7 \pm 2.7$	
	$f_0(1370)$	$E_r$		$1353.8 \pm 27.9$	$1336.7 \pm 14.1$
		$\Gamma_r/2$		$367.4 \pm 37.4$	$251.9 \pm 27.5$
$f_0(1500)$	$E_r$		$1499.5 \pm 6.0$	$1500.3 \pm 6.3$	
	$\Gamma_r/2$		$56.5 \pm 6.1$	$57.0 \pm 6.4$	
$f'_0(1500)$	$E_r$	$1528.4 \pm 12.5$	$1491.3 \pm 15.8$	$1510.8 \pm 29.1$	$1515.6 \pm 17.0$
	$\Gamma_r/2$	$328.0 \pm 20.2$	$217.9 \pm 8.0$	$388.3 \pm 16.3$	$340.3 \pm 34.9$
$f_0(1710)$	$E_r$		$1703.1 \pm 31.5$		$1722.0 \pm 35.7$
	$\Gamma_r/2$		$81.7 \pm 19.9$		$92.3 \pm 20.3$

chiral approaches based on the linear realization of chiral symmetry (models of the Nambu–Jona-Lasinio (NJL) type [22, 23]). Taking into account very precise experiments at CERN performed by the NA48/2 Collaboration [24] and the DIRAC Collaboration [25], which confirmed the prediction of the ChPT [21, 9] one ought to prefer the A-solution. In particular, the NA48/2 Collaboration [24] extracted the  $S$ -wave  $\pi\pi$  scattering lengths

$$\begin{aligned}
a_0^0 &= (0.2220 \pm 0.0128_{\text{stat}} \pm 0.0050_{\text{syst}} \pm 0.0037_{\text{th}}) m_{\pi^+}^{-1} \\
a_2^0 &= (-0.0432 \pm 0.0086_{\text{stat}} \pm 0.0034_{\text{syst}} \pm 0.0028_{\text{th}}) m_{\pi^+}^{-1}
\end{aligned} \tag{3.8}$$

from the analysis of the  $K_{e4}$  decay  $K^\pm \rightarrow \pi^+\pi^-e^\pm\nu$ . The DIRAC Collaboration extracted the

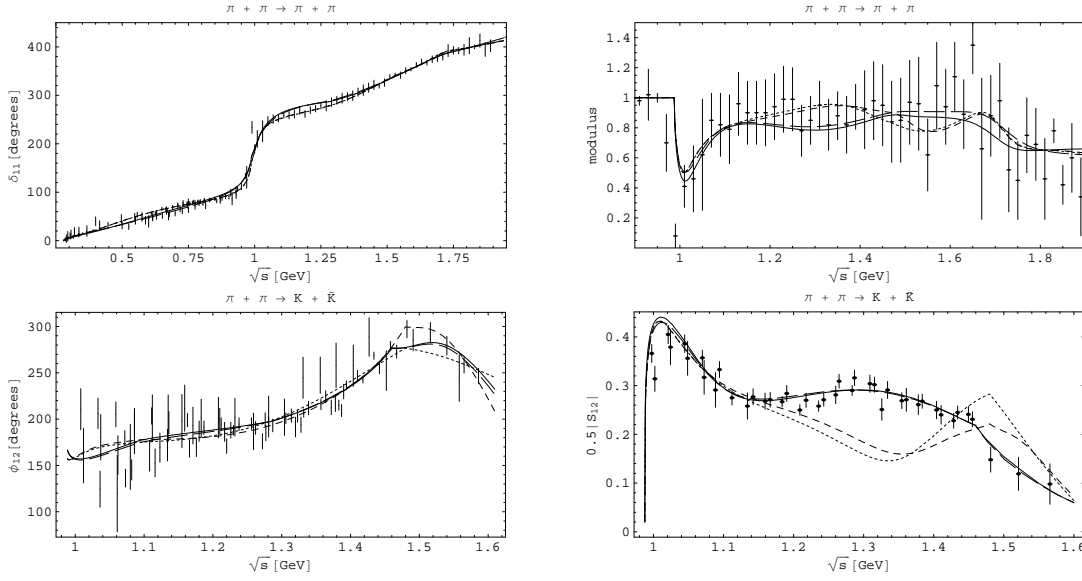


**Figure 2:** The  $S$ -wave phase shifts and modules of the  $\pi\pi$ -scattering and  $\pi\pi \rightarrow K\bar{K}$  matrix elements. The dotted and short-dashed lines correspond to the analyses only of  $\pi\pi$ -scattering without and with the narrow  $f_0(1500)$ , respectively; in the lower row those curves give energy behaviour of the phase shift and module of the  $\pi\pi \rightarrow K\bar{K}$  matrix element which are calculated using the resonance parameters from the analysis of only  $\pi\pi$ -scattering. The long-dashed and solid lines correspond to solutions A and B of the combined analysis of  $\pi\pi \rightarrow \pi\pi, K\bar{K}$ , respectively.

**Table 4:** The  $\pi\pi$  scattering length  $a_0^0$ .

$a_0^0 [m_{\pi^+}^{-1}]$	Remarks	References
$0.222 \pm 0.008$	Analysis only of $\pi\pi$ scattering	This paper
$0.230 \pm 0.004$	A-solution	This paper: combined analysis of processes $\pi\pi \rightarrow \pi\pi, K\bar{K}$
$0.282 \pm 0.003$	B-solution	
$0.26 \pm 0.05$	Analysis of the $K \rightarrow \pi\pi e\nu$ using Roy's equation	L.Rosselet et al. (1977) [17]
$0.24 \pm 0.09$	Analysis of $\pi^- p \rightarrow \pi^+ \pi^- n$ using the effective range formula	A.A.Bel'kov et al. (1979) [17]
$0.2220 \pm 0.0128_{\text{stat}} \pm 0.0050_{\text{syst}} \pm 0.0037_{\text{th}}$	Experiment on $K_{e4}$ decay	J.R.Batley et al. (2010) [24]
$0.220 \pm 0.005$	ChPT + Roy's equations	G.Colangelo et al., PL B (2000) [9, 21]
$0.220 \pm 0.008$	Dispersion relations and $K_{e4}$ data	R.García-Martín et al. (2011) [10]
0.26	NJL model (I)	M.K.Volkov (1986) [22]
0.28	NJL model (II)	A.N.Ivanov, N.I.Troitskaya (1995) [23]

quantity

$$|a_0^0 - a_2^0| = \left( 0.2533_{-0.0078}^{+0.0080} \Big|_{\text{stat}} \begin{array}{c} +0.0078 \\ -0.0073 \end{array} \Big|_{\text{syst}} \right) m_{\pi^+}^{-1} \quad (3.9)$$

from the measurement of the  $\pi^+\pi^-$  atom lifetime  $\tau$  in the ground state using the model-independent formula derived in Refs. [26] at next-to-leading order (NLO) in isospin breaking:

$$\tau^{-1} \sim (a_0^0 - a_2^0)^2 (1 + \delta), \quad (3.10)$$

where the quantity  $\delta = (5.8 \pm 1.2) \times 10^{-2}$  encodes the NLO isospin-breaking correction.

One can see that *in the combined analysis of data on coupled processes both above-indicated important flaws, related to the analysis of only  $\pi\pi$ -scattering, are cured.*

Now the  $\pi\pi$  background below the  $K\bar{K}$  threshold is absent ( $a_{11} = 0.0$ ) because its contribution is practically completely accounted for by the left-hand branch-point at  $s = 0$  included explicitly in the uniformizing variable. An arising pseudo-background at the  $\eta\eta$  threshold ( $a_{1\eta} < 0$ ) is also clear: *this is a direct indication to consider explicitly the  $\eta\eta$ -threshold branch-point.* This was already done in our work [7]. The 3-channel combined analysis of data on processes  $\pi\pi \rightarrow \pi\pi, K\bar{K}, \eta\eta(\eta\eta')$  was carried out. As in the above 2-channel combined analysis, two solutions (A and B), mainly related with parameters of the  $f_0(600)$ , were found. Furthermore, it was shown that there are four scenarios of representation of resonances  $f_0(1370)$ ,  $f_0(1500)$  (as the superposition of two states, broad and narrow) and  $f_0(1710)$  giving the similar description of the above processes and, however, the quite different parameters of some resonances. For the  $f_0(600)$ ,  $f_0(1370)$  and  $f_0(1710)$ , a spread of values was obtained for the masses and widths 605-735 and 567-686 MeV, 1326-1404 and 223-345 MeV, and 1751-1759 and 118-207 MeV, respectively. The  $f_0(600)$  and  $f_0(980)$  are given by the pole clusters of the same types in all cases.

*In order to diminish the number of possible scenarios, it is required to enlarge the analysis adding data on the relevant decays.*

#### 4. The combined 3-channel analysis of data on isoscalar S-wave processes

$\pi\pi \rightarrow \pi\pi, K\bar{K}, \eta\eta$  and on decays  $J/\psi \rightarrow \phi\pi\pi, \phi K\bar{K}$

Enlarging our analysis, to the data on processes  $\pi\pi \rightarrow \pi\pi, K\bar{K}, \eta\eta$  we added also data on decays  $J/\psi \rightarrow \phi\pi\pi, \phi K\bar{K}$  from Mark III, DM2, and BES Collaborations [13].

The 3-channel  $S$ -matrix is determined on the 8-sheeted Riemann surface. That function can be uniformized only on torus with the help of a simple mapping. This is unsatisfactory for our purpose. Therefore, we neglect the influence of the lowest ( $\pi\pi$ ) threshold branch-point (however, unitarity on the  $\pi\pi$  cut is taken into account). This approximation means the consideration of the nearest to the physical region semi-sheets of the Riemann surface of the  $S$ -matrix. In fact, we construct a 4-sheeted model of the initial 8-sheeted Riemann surface that is in accordance with our approach of a consistent account of the nearest singularities on all the relevant sheets.

In the corresponding uniformizing variable, we have neglected the  $\pi\pi$ -threshold branch-point and taken into account the  $K\bar{K}$ - and  $\eta\eta$ -threshold branch-points and the left-hand branch-point at  $s = 0$ :

$$w = \frac{\sqrt{(s-s_2)s_3} + \sqrt{(s-s_3)s_2}}{\sqrt{s(s_3-s_2)}} \quad (s_2 = 4m_K^2 \text{ and } s_3 = 4m_\eta^2). \quad (4.1)$$

This variable maps our model of the 8-sheeted Riemann surface onto the  $w$ -plane divided into two parts by a unit circle centered at the origin. The semi-sheets I (III), II (IV), V (VII) and VI (VIII) are mapped onto the exterior (interior) of the unit disk in the 1st, 2nd, 3rd and 4th quadrants, respectively. The physical region extends from the point  $\pi\pi$  on the imaginary axis (the first  $\pi\pi$  threshold corresponding to  $s_1$ ) along this axis down to the point  $i$  on the unit circle (the second threshold corresponding to  $s_2$ ). Then it extends further along the unit circle clockwise in the 1st quadrant to point 1 on the real axis (the third threshold corresponding to  $s_3$ ) and then along the real axis to the point  $b = (\sqrt{s_2} + \sqrt{s_3})/\sqrt{s_3 - s_2}$  into which  $s = \infty$  is mapped on the  $w$ -plane. The intervals  $(-\infty, -b]$ ,  $[-b^{-1}, b^{-1}]$ ,  $[b, \infty)$  on the real axis are the images of the corresponding edges of the left-hand cut of the  $\pi\pi$ -scattering amplitude. In Fig.3, the 3-channel resonances of types (a), (b), (c) and (g) in  $S_{11}(w)$ , met in this analysis, are represented by the poles (\*) and zeroes (o) symmetric to these poles with respect to the imaginary axis giving corresponding pole clusters.

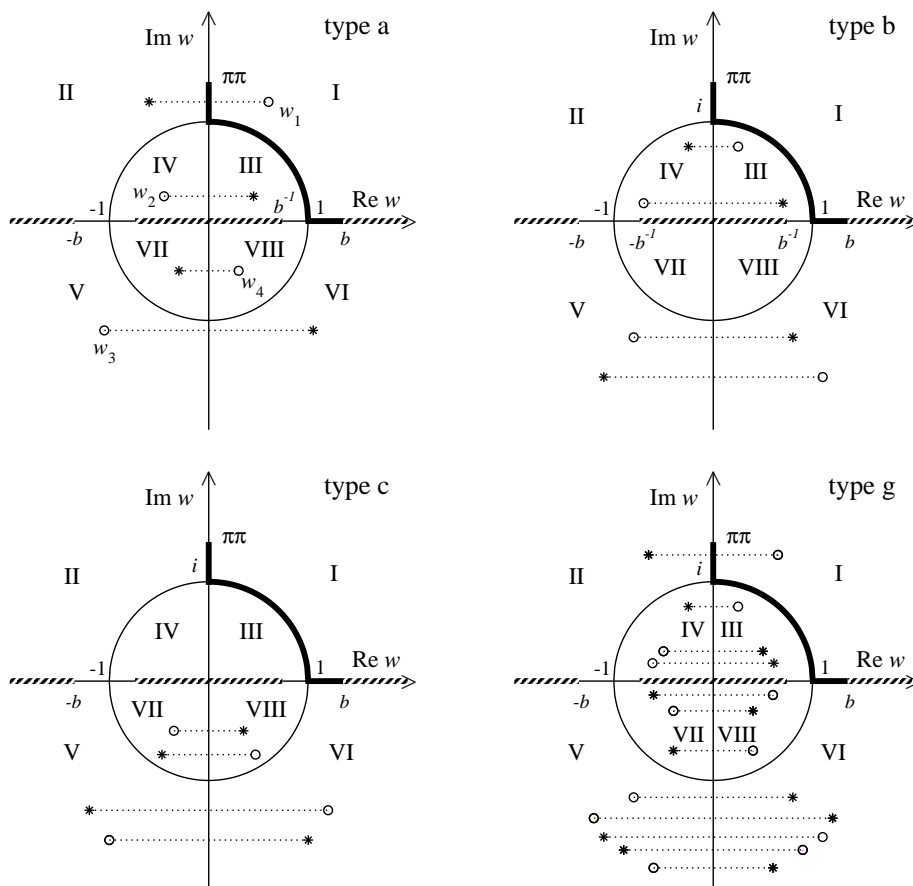


**Figure 3:** Uniformization  $w$ -plane for the 3-channel- $\pi\pi$ -scattering amplitude: Representation of resonances of types (a), (b), (c) and (g).

On the  $w$ -plane, the Le Couteur-Newton relations are

$$\begin{aligned} S_{11} &= \frac{d^*(-w^*)}{d(w)}, & S_{22} &= \frac{d(-w^{-1})}{d(w)}, & S_{33} &= \frac{d(w^{-1})}{d(w)}, \\ S_{11}S_{22} - S_{12}^2 &= \frac{d^*(w^{*-1})}{d(w)}, & S_{11}S_{33} - S_{13}^2 &= \frac{d^*(-w^{*-1})}{d(w)}, \end{aligned} \quad (4.2)$$

where the  $d$ -function is taken as

$$d = d_B d_{res} \quad (4.3)$$

with the following resonance part

$$d_{res}(w) = w^{-\frac{M}{2}} \prod_{r=1}^M (w + w_r^*) \quad (4.4)$$

( $M$  is the number of resonance zeros) and the background part

$$d_B = \exp\left[-i\left(a + \sum_{n=1}^3 \frac{\sqrt{s-s_n}}{2m_n} (\alpha_n + i\beta_n)\right)\right], \quad (4.5)$$

where

$$\begin{aligned} \alpha_n &= a_{n1} + a_{n\sigma} \frac{s-s_\sigma}{s_\sigma} \theta(s-s_\sigma) + a_{nv} \frac{s-s_v}{s_v} \theta(s-s_v), \\ \beta_n &= b_{n1} + b_{n\sigma} \frac{s-s_\sigma}{s_\sigma} \theta(s-s_\sigma) + b_{nv} \frac{s-s_v}{s_v} \theta(s-s_v). \end{aligned}$$

Here  $s_\sigma$  is the  $\sigma\sigma$  threshold;  $s_v$  is the combined threshold of the  $\eta\eta'$ ,  $\rho\rho$ ,  $\omega\omega$  channels.

Formalism for calculating di-meson mass distributions of the decays  $J/\psi \rightarrow \phi\pi\pi, \phi K\bar{K}$  can be found in Refs. [15, 27, 28]. There is assumed that pairs of pseudo-scalar mesons of final states have  $I = J = 0$  and only they undergo strong interactions, whereas the  $\phi$  meson acts as a spectator.

The amplitudes for  $J/\psi \rightarrow \phi\pi\pi, \phi K\bar{K}$  decays are related with the scattering amplitudes  $T_{ij}$   $i, j = 1 - \pi\pi, 2 - K\bar{K}$  as follows

$$F(J/\psi \rightarrow \phi\pi\pi) = \sqrt{2/3} [c_1(s)T_{11} + c_2(s)T_{21}], \quad (4.6)$$

$$F(J/\psi \rightarrow \phi K\bar{K}) = \sqrt{1/2} [c_1(s)T_{12} + c_2(s)T_{22}] \quad (4.7)$$

where  $c_i = \alpha_i/(s - \beta_i) + \gamma_{i0} + \gamma_{i1}s$  are functions of couplings of the  $J/\psi$  to channel  $i$ ;  $\alpha_i, \beta_i, \gamma_{i0}$  and  $\gamma_{i1}$  are free parameters. The first term in  $c_i$  is related to the on-shell manifestation of Adler zero. The formula

$$N|F|^2 \sqrt{(s-s_i)(m_\psi^2 - (\sqrt{s} - m_\phi)^2)(m_\psi^2 - (\sqrt{s} + m_\phi)^2)} \quad (4.8)$$

gives the di-meson mass distributions.  $N$  (normalization to experiment) is 0.73 for Mark III and 0.28 for DM2 and 5.65 for BES data. Parameters of the  $c_i$ -functions, obtained in the analysis, are  $\alpha_1, \beta_1, \alpha_2, \beta_2 = 0.0306, 0.0646, 0.0222, 0.0701$ ;  $\gamma_{10}, \gamma_{11}, \gamma_{20}, \gamma_{21} = 1.6148, 1.3169, -1.0962, -1.64$ .

In the analysis the  $f_0(600)$  is described by the cluster of type **(a)**;  $f_0(1500)$ , type **(c)** and  $f_0'(1500)$ , type **(g)**; the  $f_0(980)$  is represented only by the pole on sheet II and shifted pole on sheet III and by the corresponding zeros on sheets II and IV. However, the  $f_0(1370)$  and  $f_0(1710)$

can be described by clusters either of type **(b)** or **(c)**. Analyzing only  $\pi\pi \rightarrow \pi\pi, K\bar{K}, \eta\eta(\eta\eta')$  [7], it is impossible to prefer surely any of four indicated possibilities; moreover, the data admit two possibilities for parameters of the  $f_0(600)$  with mass, relatively near to the  $\rho$ -meson mass, and with the total widths about 600 and 950 MeV.

When adding to the combined analysis the data on decays  $J/\psi \rightarrow \phi\pi\pi, \phi K\bar{K}$ , one can give some preference for the scenarios when the  $f_0(1370)$  is described by the cluster of type **(b)**,  $f_0(1710)$  either of type **(b)** or **(c)**. Further, for definiteness, we shall tell about the case when the  $f_0(1710)$  is represented by the cluster of type **(c)**.

It is interesting that *the di-pion mass distribution in the  $J/\psi \rightarrow \phi\pi\pi$  decay of the BES data from the threshold to about 0.85 GeV prefers surely the solution with the more wide  $f_0(600)$  – B-solution*. Satisfactory combined description of all analyzed processes is obtained with the total  $\chi^2/\text{NDF} = 424.317/(389 - 55) \approx 1.26$ : for the  $\pi\pi$  scattering,  $\chi^2/\text{NDF} \approx 1.20$ ; for  $\pi\pi \rightarrow K\bar{K}$ ,  $\chi^2/\text{NDF} \approx 1.64$ ; for  $\pi\pi \rightarrow \eta\eta$ ,  $\chi^2/\text{ndp} \approx 0.82$ ; for decays  $J/\psi \rightarrow \phi\pi\pi, \phi K\bar{K}$ ,  $\chi^2/\text{NDF} \approx 1.55$ .

In Figures 4, 5 and 6, we show results of fitting (B-solution) to the analyzed experimental data.

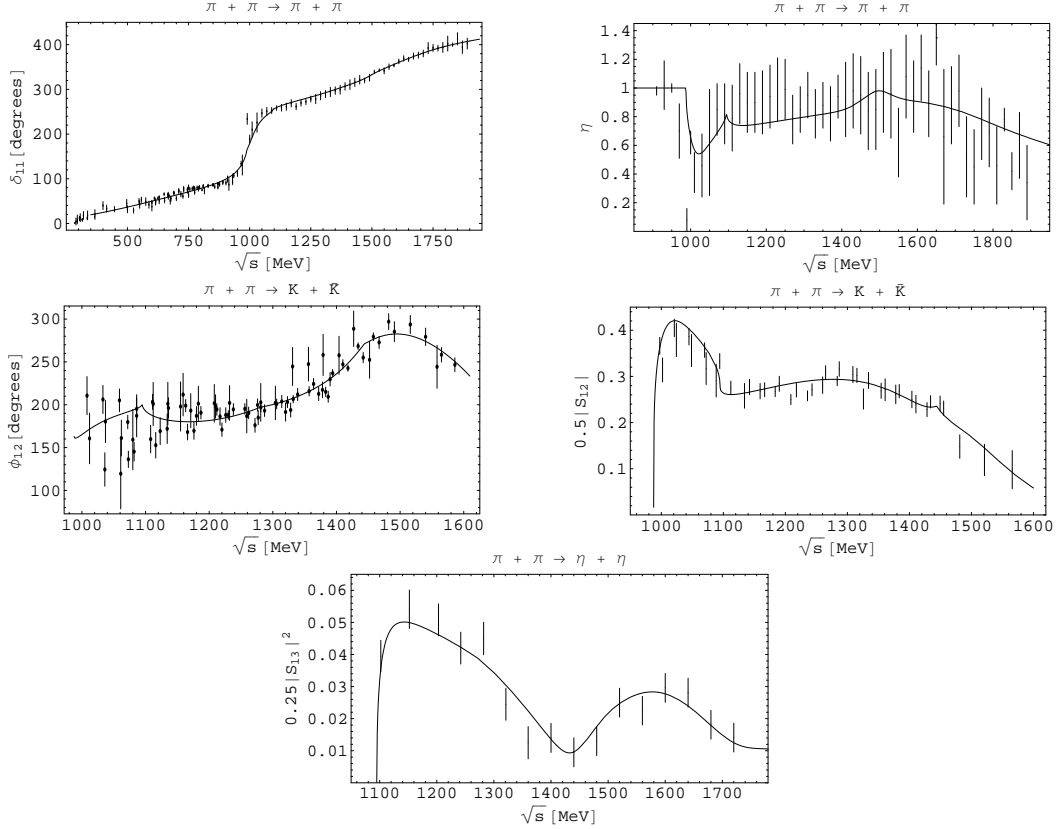


**Figure 4:** The phase shifts and modules of the  $S$ -wave  $S$ -matrix elements in the  $\pi\pi$ -scattering (upper panel) and  $\pi\pi \rightarrow K\bar{K}$  (middle panel), and the squared modulus of the  $\pi\pi \rightarrow \eta\eta$   $S$ -wave matrix element (lower figure). The data are from Refs. [17, 18, 19].

The obtained background parameters are:

$$a_{11} = 0.0, a_{1\sigma} = 0.0198, a_{1\nu} = 0.0, b_{11} = b_{1\sigma} = 0.0, b_{1\nu} = 0.0336, a_{21} = -2.4808, a_{2\sigma} = -2.3021,$$

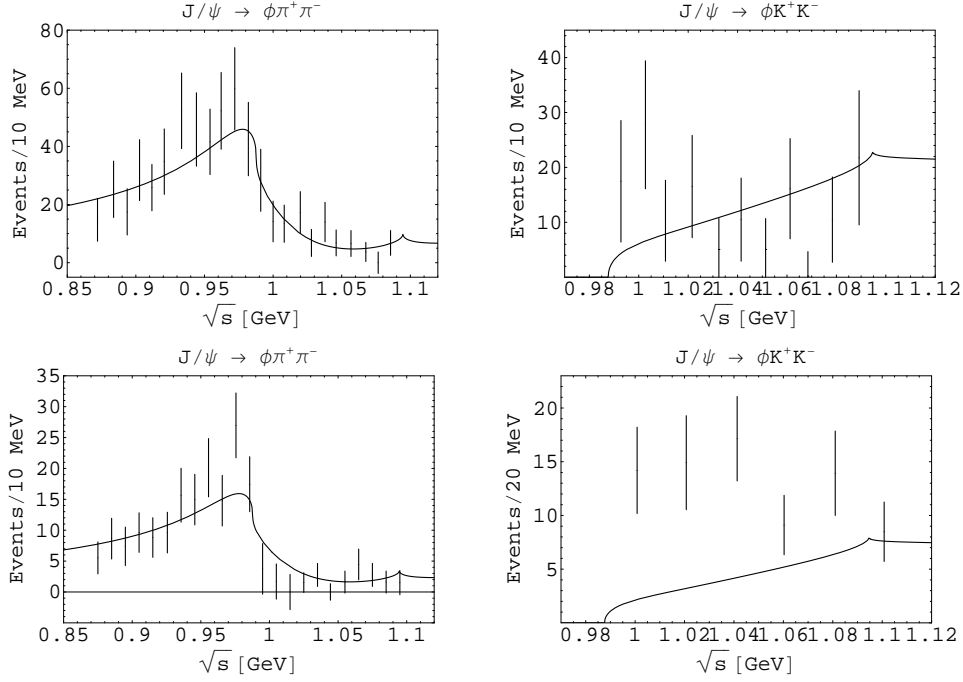


**Figure 5:** The  $J/\psi \rightarrow \phi\pi\pi, \phi K\bar{K}$  decays. The upper panel shows the fit to data of Mark III, the lower to DM2.

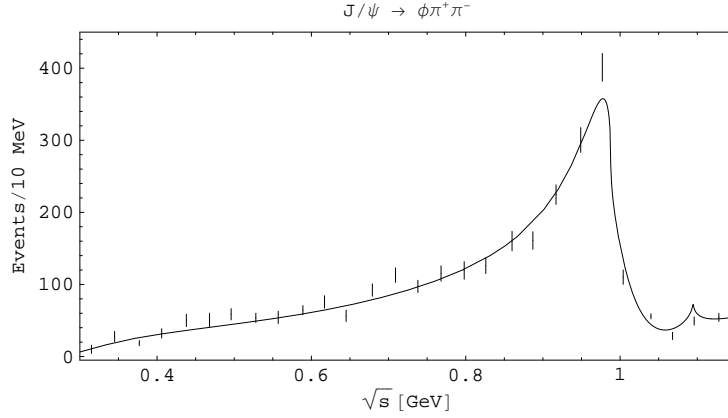


**Figure 6:** The  $J/\psi \rightarrow \phi\pi\pi$  decay; the data of BES Collaboration.

$a_{2v} = -6.62, b_{21} = b_{2\sigma} = 0.0, b_{2v} = 6.99, b_{31} = 0.6432, b_{3\sigma} = 0.489, b_{2v} = 0; s_{\sigma} = 1.6384 \text{ GeV}^2, s_v = 2.0851 \text{ GeV}^2.$

The obtained very simple description of the  $\pi\pi$ -scattering background confirms well our assumption:  $d = d_B d_{res}$ . Moreover, this shows that *the consideration of the left-hand branch-point at  $s = 0$  in the uniformizing variable solves partly a problem (see, e.g., [29]) that the wide-resonance parameters are strongly controlled by the non-resonant background.*

In Table 4 we indicate the obtained pole clusters (B-solution) for resonances on the eight sheets in the complex energy plane  $\sqrt{s}$ . The poles, corresponding to the  $f_0'(1500)$ , on sheets III,

V and VII are of the 2nd order and that on the sheet VI of the 3rd order in our approximation. Generally, *wide multi-channel states are most adequately represented by pole clusters*, because the

**Table 5:** The pole clusters for resonances (B-solution) on the  $\sqrt{s}$ -plane.  $\sqrt{s_r} = E_r - i\Gamma_r/2$  [MeV].

Sheet		$f_0(600)$	$f_0(980)$	$f_0(1370)$	$f_0(1500)$	$f'_0(1500)$	$f_0(1710)$
II	$E_r$	$521.6 \pm 12.4$	$1008.4 \pm 3.1$			$1512.4 \pm 4.9$	
	$\Gamma_r/2$	$467.3 \pm 5.9$	$33.5 \pm 1.5$			$287.2 \pm 12.9$	
III	$E_r$	$552.5 \pm 17.7$	$976.7 \pm 5.8$	$1387.2 \pm 24.4$		$1506.1 \pm 9.0$	
	$\Gamma_r/2$	$467.3 \pm 5.9$	$53.2 \pm 2.6$	$167.2 \pm 41.8$		$127.8 \pm 10.6$	
IV	$E_r$			$1387.2 \pm 24.4$		$1512.4 \pm 4.9$	
	$\Gamma_r/2$			$178.2 \pm 37.2$		$215.0 \pm 17.6$	
V	$E_r$			$1387.2 \pm 24.4$	$1493.9 \pm 3.1$	$1498.8 \pm 7.2$	$1732.8 \pm 43.2$
	$\Gamma_r/2$			$261.0 \pm 73.7$	$72.8 \pm 3.9$	$142.3 \pm 6.0$	$114.8 \pm 61.5$
VI	$E_r$	$573.4 \pm 29.1$		$1387.2 \pm 24.4$	$1493.9 \pm 5.6$	$1511.5 \pm 4.3$	$1732.8 \pm 43.2$
	$\Gamma_r/2$	$467.3 \pm 5.9$		$250.0 \pm 83.1$	$58.4 \pm 2.8$	$179.3 \pm 4.0$	$111.2 \pm 8.8$
VII	$E_r$	$542.5 \pm 25.5$			$1493.9 \pm 5.0$	$1500.4 \pm 9.3$	$1732.8 \pm 43.2$
	$\Gamma_r/2$	$467.3 \pm 5.9$			$47.8 \pm 9.3$	$99.9 \pm 18.0$	$55.2 \pm 38.0$
VIII	$E_r$				$1493.9 \pm 3.2$	$1512.4 \pm 4.9$	$1732.8 \pm 43.2$
	$\Gamma_r/2$				$62.2 \pm 9.2$	$298.4 \pm 14.5$	$58.8 \pm 16.4$

pole clusters give the main model-independent effect of resonances. The pole positions are rather stable characteristics for various models, whereas masses and widths are very model-dependent for wide resonances.

However, mass values are needed in some cases, e.g., in mass relations for multiplets. Therefore, we stress that such parameters of the wide multi-channel states, as *masses, widths and coupling constants with channels, should be calculated using the poles on sheets II, IV, VIII*, because only on these sheets the analytic continuations have the forms:

$$\propto 1/S_{11}^I, \quad \propto 1/S_{22}^I, \quad \propto 1/S_{33}^I,$$

respectively, i.e., the pole positions of resonances are at the same points of the complex-energy plane, as the resonance zeros on the physical sheet, and are not shifted due to the coupling of channels. E.g., if the resonance part of the amplitude is taken as

$$T^{res} = \frac{\sqrt{s}\Gamma_{el}}{m_{res}^2 - s - i\sqrt{s}\Gamma_{tot}} \quad (4.9)$$

we obtain the formulas

$$m_{res} = \sqrt{E_r^2 + (\Gamma_r/2)^2} \quad \text{and} \quad \Gamma_{tot} = \Gamma_r, \quad (4.10)$$

where the pole position  $\sqrt{s_r} = E_r - i\Gamma_r/2$  must be taken on sheets II, IV, VIII, depending on the resonance classification. In Table 6 there are given the obtained masses and total widths of states, calculated from the pole positions on sheets II, IV and VIII for resonances of types (a), (b) and (c), respectively.

**Table 6:** The masses and total widths (in MeV) of the  $f_0$  resonances in the B solution.

	$f_0(600)$	$f_0(980)$	$f_0(1370)$	$f_0(1500)$	$f_0'(1500)$	$f_0(1710)$
$m_{res}$ [MeV]	$700.3 \pm 10.0$	$1009.0 \pm 3.1$	$1398.6 \pm 24.7$	$1495.2 \pm 3.2$	$1539.4 \pm 5.4$	$1733.8 \pm 43.2$
$\Gamma_{tot}$ [MeV]	$934.6 \pm 11.8$	$67.0 \pm 3.0$	$356.4 \pm 74.4$	$124.4 \pm 18.4$	$574.4 \pm 25.8$	$117.6 \pm 32.8$

## 5. Discussion and conclusions

- The Riemann-surface structure of the  $S$ -matrix of considered processes must be allowed for properly. For calculating masses, total widths and coupling constants of resonances with channels, one must use the poles on sheets II, IV and VIII, depending on the resonance type.
- When considering the  $\pi\pi$  scattering and  $\pi\pi \rightarrow K\bar{K}$  in the 2-channel approach, it is shown that the analysis of only  $\pi\pi$  scattering data, gives an excellent description from the threshold to 1.89 GeV with the resonance parameters and  $\pi\pi$ -scattering length being the same as the ones indicated in the PDG tables as estimations. However, (1) the  $\pi\pi \rightarrow K\bar{K}$  are not well described even qualitatively above 1.15 GeV when using the resonance parameters from the only  $\pi\pi$  scattering analysis, and (2) in this case, the description of  $\pi\pi$  background is unsatisfactory (pseudo-background arises). I.e., a combined analysis of  $\pi\pi \rightarrow \pi\pi, K\bar{K}$  is needed, which also is carried out satisfactorily, curing flaws (1) and partly (2). The resonance parameters are inevitably changed. The remaining pseudo-background arising at the  $\eta\eta$  threshold indicates clearly that it is necessary to consider explicitly also the  $\eta\eta$ -threshold branch-point in the 3-channel analysis.
- If a state decays into several channels, then, obviously, it must be studied in a multi-channel approach. Here it is shown that even if some channels are energetically-closed for the state which, however, is strongly coupled with these channels (this coupling is displayed in exchanges in the crossed channels), then this state should be considered on the Riemann surface where the sheets are taken into account, which arise due to the threshold branch-points of these energetically-closed channels. Moreover in order to obtain correct values of the state parameters, it is necessary to perform the combined analysis of all relevant coupled processes.
- In the combined model-independent analysis of data on  $\pi\pi \rightarrow \pi\pi, K\bar{K}, \eta\eta$  and on  $J/\psi \rightarrow \phi\pi\pi, \phi K\bar{K}$  from Mark III, DM2 and BES Collaborations, an additional confirmation of the  $f_0(600)$  with mass about 700 MeV and width 930 MeV is obtained. This mass value accords with prediction ( $m_\sigma \approx m_\rho$ ) on the basis of mended symmetry by Weinberg [30] and with a refined analysis using the large- $N_c$  consistency conditions between the unitarization and resonance saturation suggesting  $m_\rho - m_\sigma = O(N_c^{-1})$  [31].
- Indication for  $f_0(980)$  is obtained to be a non- $q\bar{q}$  state, e.g., the bound  $\eta\eta$  state, because this state lies slightly above the  $K\bar{K}$  threshold and is described by the pole on sheet II and by the shifted pole on sheet III without the corresponding poles on sheets VI and VII.

- The  $f_0(1370)$  and  $f_0(1710)$  have the dominant  $s\bar{s}$  component. Conclusion about the  $f_0(1370)$  quite agrees with the one of work of Crystal Barrel Collaboration [32] where the  $f_0(1370)$  is identified as  $\eta\eta$  resonance in the  $\pi^0\eta\eta$  final state of the  $\bar{p}p$  annihilation. This explains also quite well why one did not find this state considering only the  $\pi\pi$  scattering [33, 34]. Conclusion about the  $f_0(1710)$  is consistent with the experimental facts that this state is observed in  $\gamma\gamma \rightarrow K_S K_S$  [35] and not observed in  $\gamma\gamma \rightarrow \pi^+\pi^-$  [36].
- In the 1500-MeV region, there are two states: the  $f_0(1500)$  ( $m_{res} \approx 1495$  MeV,  $\Gamma_{tot} \approx 124$  MeV) and the  $f'_0(1500)$  ( $m_{res} \approx 1539$  MeV,  $\Gamma_{tot} \approx 574$  MeV). The  $f'_0(1500)$  is interpreted as a glueball taking into account its biggest width among enclosing states [37].
- We propose the following assignment of the scalar mesons to lower nonets, excluding the  $f_0(980)$  as the non- $q\bar{q}$  state. The lowest nonet: the isovector  $a_0(980)$ , the isodoublet  $K_0^*(800)$ , and  $f_0(600)$  and  $f_0(1370)$  as mixtures of the 8th component of octet and the SU(3) singlet. The Gell-Mann–Okubo (GM-O) formula

$$3m_{f_8}^2 = 4m_{K_0^*}^2 - m_{a_0}^2$$

gives  $m_{f_8} = 870$  MeV. In relation for masses of nonet

$$m_\sigma + m_{f_0(1370)} = 2m_{K_0^*(800)}$$

the left-hand side is by about 17% bigger than the right-hand one.

- For the next nonet we find: the isovector  $a_0(1450)$ , the isodoublet  $K_0^*(1450)$ , and two isoscalars  $f_0(1500)$  and  $f_0(1710)$ . From the GM-O formula,  $m_{f_8} \approx 1450$  MeV. In formula

$$m_{f_0(1500)} + m_{f_0(1710)} = 2m_{K_0^*(1450)}$$

the left-hand side is by about 11% bigger than the right-hand one.

- This assignment removes a number of questions, stood earlier, and does not put any new. The mass formulas indicate to non-simple mixing scheme. The breaking of 2nd mass relations tells us that the  $\sigma - f_0(1370)$  and  $f_0(1500) - f_0(1710)$  systems get additional contributions absent in the  $K_0^*(900)$  and  $K_0^*(1450)$ , respectively. A search of the adequate mixing scheme is complicated by the fact that here there is also a remaining chiral symmetry, though, on the other hand, this permits one to predict correctly, e.g., the  $\sigma$ -meson mass [30].

## 6. Acknowledgments

This work was supported in part by the Heisenberg-Landau Program, the RFBR grant 10-02-00368-a, the Votruba-Blokhintsev Program for Cooperation of Czech Republic with JINR (Dubna), the Grant Agency of Czech Republic (Grant No. P203/12/2126), the Grant Program of Plenipotentiary of Slovak Republic at JINR, the Slovak Scientific Grant Agency (Grant VEGA No.2/0034/09), the Bogoliubov-Infeld Program for Cooperation of Poland with JINR, by the DFG under Contract No. LY 114/2-1 and by Federal Targeted Program “Scientific and scientific-pedagogical personnel of innovative Russia” Contract No. 02.740.11.0238. This work has been partly supported by the Polish Ministry of Science and Higher Education (grant No N N202 101 368).

## References

- [1] K. Nakamura *et al.* (Particle Data Group), J. Phys. G **37**, 075021 (2010).
- [2] J. Beringer *et al.* (PDG), Phys. Rev. D **86**, 010001 (2012).
- [3] C. Amsler and N. A. Tornqvist, Phys. Rept. **389**, 61 (2004).
- [4] D. V. Bugg, Phys. Rep. **397**, 257 (2004).
- [5] F. E. Close and N. A. Tornqvist, J. Phys. G **28**, R249 (2002). **28**, R249 (2002).
- [6] E. Klempt and A. Zaitsev, Phys. Rep. **454**, 1 (2007).
- [7] Yu.S. Surovtsev, P. Bydžovský, and V.E. Lyubovitskij, Phys. Rev. D **85**, 036002 (2012).
- [8] Yu.S. Surovtsev, P. Bydžovský, R. Kamiński, and M. Nagy, Phys. Rev. D **81**, 016001 (2010).
- [9] G. Colangelo, J. Gasser and H. Leutwyler, Nucl. Phys. B **603**, 125 (2001); B. Ananthanarayan, G. Colangelo, J. Gasser and H. Leutwyler, Phys. Rep. **353**, 207 (2001).
- [10] R. García-Martín, R. Kamiński, J.R. Peláez, and F.J. Ynduráin, Phys. Rev. D **83**, 074004 (2011).
- [11] I. Caprini, G. Colangelo, and H. Leutwyler, Phys. Rev. Lett. **96**, 132001 (2006).
- [12] R. García-Martín, R. Kamiński, R. Peláez, and J. Ruiz de Elvira, Phys. Rev. Lett. **107**, 072001 (2011).
- [13] W. Lockman, Hadron'89, Proceedings, p.109; A. Falvard *et al.*, Phys. Rev. D **38**, 2706 (1988); M. Ablikim *et al.*, Phys. Lett. B **607**, 243 (2005).
- [14] D. Krupa, V.A. Meshcheryakov, and Yu.S. Surovtsev, Nuovo Cim. A **109**, 281 (1996).
- [15] D. Morgan and M.R. Pennington, Phys. Rev. D **48**, 1185 (1993).
- [16] K.J. Le Couteur, Proc. R. London, Ser. A **256**, 115 (1960); R.G. Newton, J. Math. Phys. **2**, 188 (1961); M. Kato, Ann. Phys. **31**, 130 (1965).
- [17] J.R. Batley *et al.*, Eur. Phys. J. C **54** (2008) 411; B. Hyams *et al.*, Nucl. Phys. B **64**, 134 (1973); **100**, 205 (1975); A. Zylbersztejn *et al.*, Phys. Lett. B **38**, 457 (1972); P. Sonderegger, P. Bonamy, in Proc. 5th Int. Conference on Elementary Particles, Lund, 1969, 372; J.R. Bensinger *et al.*, Phys. Lett. B **36**, 134 (1971); J.P. Baton *et al.*, Phys. Lett. B **33**, 525 (1970); **33**, 528 (1970); P. Baillon *et al.*, Phys. Lett. B **38**, 555 (1972); L. Rosselet *et al.*, Phys. Rev. D **15**, 574 (1977); A.A. Kartamyshev *et al.*, Pis'ma Zh. Eksp. Theor. Fiz. **25**, 68 (1977); A.A. Bel'kov *et al.*, Pis'ma Zh. Eksp. Theor. Fiz. **29**, 652 (1979); S.D. Protopopescu *et al.*, Phys. Rev. D **7**, 1279 (1973); P. Estabrooks and A.D. Martin, Nucl. Phys. B **79**, 301 (1974).
- [18] W. Wetzel *et al.*, Nucl. Phys. B **115**, 208 (1976); V.A. Polychronakos *et al.*, Phys. Rev. D **19**, 1317 (1979); P. Estabrooks, Phys. Rev. D **19**, 2678 (1979); D. Cohen *et al.*, Phys. Rev. D **22**, 2595 (1980); G. Costa *et al.*, Nucl. Phys. B **175**, 402 (1980); A. Etkin *et al.*, Phys. Rev. D **25**, 1786 (1982).
- [19] F. Binon *et al.*, Nuovo Cimento A **78**, 313 (1983).
- [20] Yu.S. Surovtsev, D. Krupa, and M. Nagy, Eur. Phys. J. A **15**, 409 (2002).
- [21] G. Colangelo, J. Gasser and H. Leutwyler, Phys. Lett. B **488**, 261 (2000).
- [22] M. K. Volkov, Sov. J. Part. Nucl. **17**, 186 (1986) [Fiz. Elem. Chast. Atom. Yadra **17**, 433 (1986)].
- [23] A.N. Ivanov and N.I. Troitskaya, Nuovo Cim. A **108**, 555 (1995).
- [24] J. R. Batley *et al.* (NA48/2 Collaboration), Eur. Phys. J. C **70**, 635 (2010).

- [25] B. Adeva, L. Afanasyev, M. Benayoun, A. Benelli, Z. Berka, V. Brekhovskikh, G. Caragheorghopol and T. Cechak *et al.*, Phys. Lett. B **704**, 24 (2011).
- [26] J. Gasser, V. E. Lyubovitskij, A. Rusetsky and A. Gall, Phys. Rev. D **64**, 016008 (2001); J. Gasser, V. E. Lyubovitskij and A. Rusetsky, Phys. Rept. **456**, 167 (2008).
- [27] D. Morgan and M.R. Pennington, Phys. Rev. D **48**, 5422 (1993).
- [28] B.S. Zou, D.V. Bugg, Phys. Rev. D **50**, 591 (1994).
- [29] N.N. Achasov and G.N. Shestakov, Phys. Rev. D **49**, 5779 (1994).
- [30] S. Weinberg, Phys. Rev. Lett. **65**, 1177 (1990).
- [31] J. Nieves and E.R. Arriola, Phys. Rev. D **80**, 045023 (2009).
- [32] C. Amsler *et al.*, Phys. Lett. **B355**, 425 (1995).
- [33] P. Minkowski and W. Ochs, Eur. Phys. J. C **9**, 283 (1999); arXiv: hep-ph/0209223; hep-ph/0209225.
- [34] W. Ochs, AIP Conf. Proc. **1257**, 252 (2010) [arXiv:1001.4486 [hep-ph]].
- [35] S. Braccini, Frascati Phys. Series **XV**, 53 (1999).
- [36] R. Barate *et al.*, Phys. Lett. B **472**, 189 (2000).
- [37] V.V. Anisovich *et al.*, Nucl. Phys. A (Proc. Suppl.) **56**, 270 (1997).